

OBSERVATIONS OF PORE SYSTEMS OF NATURAL SILICICLASTIC MUDSTONES

ANDREW C. APLIN¹ and JULIAN K.S. MOORE^{2,3}

¹*Department of Earth Sciences, Science Laboratories, South Road, Durham University, Durham, DH1 3LE, UK*

²*BP Exploration, Chertsey Road, Sunbury-on-Thames, Middlesex TW16 7LN, UK*

³*Present address: APT(UK) Ltd., 2nd Floor, Wynnstay Road, Colwyn Bay LL29 8NB, UK*

**e-mail: a.c.aplin@durham.ac.uk*

Grains within siliciclastic muds are deposited either as flocs, in which grains are generally $< \sim 10 \mu\text{m}$, or as single grains: “sortable silt,” generally $> 10 \mu\text{m}$. When clay-size ($< 2 \mu\text{m}$ diameter) particles form $> 30\%$ of mudstones, pore-size distributions are controlled mainly by the interaction of phyllosilicates; these materials are ‘matrix-supported.’ Pores associated with clay-size particles are typically $< 20 \text{nm}$, even at shallow burial. When clay-size particles comprise $< \sim 30\%$ of the grain-size distribution, a second, much larger pore system is observed, controlled by the amount and size of sortable silt; these mudstones are ‘framework-supported.’ Compaction of these silt-rich materials occurs mainly by the loss of the largest pores, but large pores still exist up to high effective stresses in the absence of chemical compaction.

Mercury injection porosimetry (MIP) gives information about pore-throat size and pore connectivity and thus provides useful data with which to estimate permeability. Models based on generally flat pore shapes can estimate the permeability of homogeneous mudstones to \pm a factor of 3 of the true value, but cannot be used for heterogeneous, laminated mudstones, which exhibit highly anisotropic permeabilities. As MIP gives information about pore throats and microscopy gives information about pore bodies, the two techniques generate different results. Both are required, along with other techniques such as small-angle neutron scattering and low-pressure gas sorption, in order to fully appreciate the complexity of mudstone pore systems.

1. Introduction

Muds mainly comprise grains $< 62.5 \mu\text{m}$ in size derived from weathering, primary production, and diagenesis. They represent a highly diverse group of rock types with mineralogies ranging from pure carbonates (*e.g.* chalk) and siliceous oozes (*e.g.* diatomites) through to volcanoclastics and siliciclastic muds that are composed primarily of clay minerals, quartz, and feldspars. Muds become mudstones, and eventually metapelites, as a result of a series of physical and chemical changes related both to increasing stress and to the thermodynamic instability of the initial mix of minerals, solutes, and organic matter – ‘burial diagenesis.’

Here, aspects of the pore systems of natural, siliciclastic muds and mudstones are considered. The significance of the mudstone pore systems is their central importance to a

wide range of practical problems relevant to fluid flow in sedimentary basins, including oil and gas production from shales, pore-pressure prediction, seal risking in petroleum systems, and CO₂ leakage from potential storage sites. The ways in which the pore systems of muds are preconditioned by their mineralogy and grain-size distribution at deposition are examined, and then how they evolve as a result of the profound physico-chemical changes that occur during subsequent burial and heating.

2. Mud deposition

The vast majority of clastic sediment is delivered to the oceans as suspended particles in rivers. Sedimentation occurs where there is insufficient energy within a fluid to keep particles in suspension. As particle settling rates are proportional to the square of particle diameter, one might expect a very marked segregation of coarse silt and clay in the marine environment as a result of settling rates which differ by orders of magnitude. However, the increasing concentration of electrolytes from river to ocean reduces the thickness of the double diffuse layers in minerals, resulting in particle flocculation or coagulation (Kranck, 1973, 1975; Eisma and Lee, 1993; Stumm and Morgan, 1995). Biological processes also cause fine-grained sediment in the water column to aggregate into composite particles. These particles are termed “organominerallic aggregates” or “marine snow” and are particularly common below regions of high primary productivity (Alldredge and Silver, 1988).

Particle-size distributions of weathered rock are poorly sorted and are fairly uniform when plotted as volumes in logarithmically increasing size classes. Models which track the evolution of fine sediment during its transport in seawater treat the suspension as a mixture of single grains and flocs (*e.g.* Kranck and Milligan, 1985; Kranck *et al.*, 1996a; Curran *et al.*, 2002), each of which has a set of hydrodynamic properties. The grain-size distribution of muds thus reflects the respective fluxes of flocs and single grains to the sediment–water interface, which in turn depends on the concentration of each component and the energy of the environment. Grain-size analyses of modern muds have been interpreted to suggest that most particles of $< \sim 10 \mu\text{m}$ are deposited as unsorted flocs, whereas larger particles (“sortable silt”) mainly settle as single grains (Kranck 1996a, 1996b; Curran *et al.*, 2002, 2004). Muddy sediments can thus be thought of as being built from two components: one which is unsorted and which comprises mainly phyllosilicate grains $< \sim 10 \mu\text{m}$, and a second which is coarser and consists mainly of quartz, mica, and feldspars (sometimes known as “sortable silt”; McCave *et al.*, 1995).

Sample grain-size distributions of two natural mudstones are shown in Figure 1. One has $\sim 70\%$ clay-size (*i.e.* $< 2 \mu\text{m}$ diameter) grains and a grain-size distribution which is both unsorted and devoid of sortable silt. The present authors infer that the grains were deposited almost entirely as flocs. The second has $\sim 25\%$ clay-size grains, has a significant amount of sortable silt, and much smaller amounts of floc-deposited grains of $< 10 \mu\text{m}$. Also shown on Figure 1 are the pore-throat size distributions of the two samples, measured by MIP. The two samples have similar porosities, $\sim 25\%$. Both samples contain pores smaller than the minimum radius that MIP can

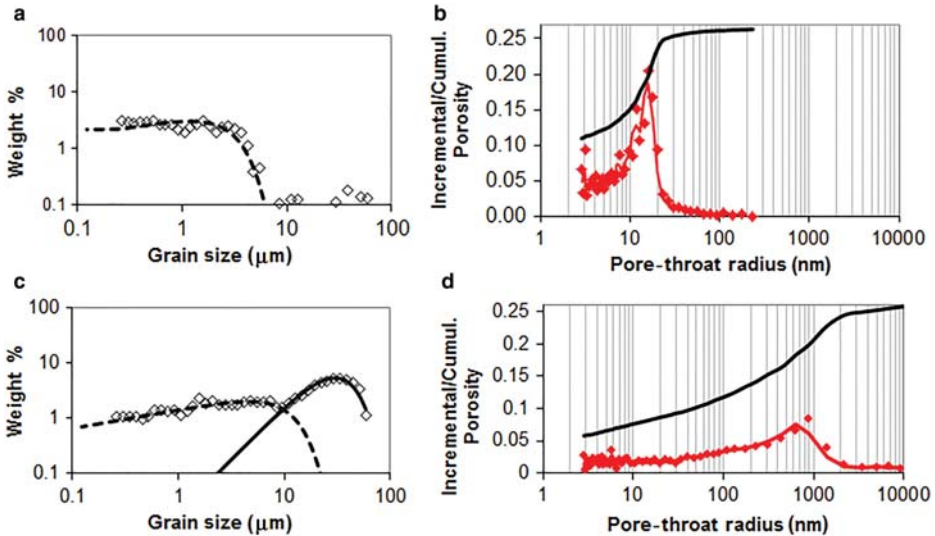


Figure 1. Grain size (left) and pore-throat size (right) distributions of two mudstones with 25% porosity. Grain-size distributions are fitted with the model of Kranck *et al.* (1996a, 1996b). The mudstone in the upper panels has a clay (<2 μm content) content of $\sim 65\%$ compared to 25% for the sample in the lower panels.

measure (~ 3 nm radius). The clay-rich sample has a modal pore size of 20 nm and no pores larger than 100 nm, however. In contrast, the silt-rich sample has a much broader pore-size distribution, with a modal pore size of 600 nm. While this qualitative relationship between grain size and pore size is to be expected, the nature of the relationship has rarely been examined in fine-grained sediments.

3. Mudstone grain and pore-size distributions

As a result of its analytical speed and wide dynamic range between 3 and 10,000 nm, MIP has probably been the most commonly used method for probing the pore-size distributions of muds and mudstones. Potential problems with MIP include the potential damage that high-pressure MIP may cause to fragile samples, and assumptions about pore shape which are inherent in the calculation of pore size. Perhaps most importantly, however, MIP measures the size of pore ‘throats,’ so that the bodies behind the throats are assigned the same radius as the throats themselves. This leads to an underestimation of pore-body size, which is important, for example, when considering fluid storage, as in gas shales. On the other hand, pore throats and their connectivity are important for considerations of fluid transport, so that MIP data can serve as a useful proxy for permeability.

While MIP-derived pore-size data for mudstones are commonly reported in the literature (*e.g.* Borst, 1982; Schlömer and Krooss, 1997; Dewhurst *et al.*, 1998, 1999a; Yang and Aplin, 1998), an understanding of what controls pore size and connectivity is much

less constrained because most reports do not include a geological description of the sample. Here, we look at MIP-derived pore-size data on samples where grain-size data were also measured. As expected, pore-size distributions at a given porosity relate to 'grain-size distributions,' but we can see that the changes in pore size seen as the samples become increasingly fine-grained/clay-rich are not linear. The data show that fundamental differences exist in muds which are either framework- or matrix-supported, and that this shift occurs when the clay content of the material is $\sim 30\text{--}35\%$.

Nagaraj *et al.* (1990) proposed that the pore systems of flocculated, fine-grained sediments comprise three pore types which can give rise to bimodal pore-size distributions. Small, intra-floc pores are created from the geometry of interlocking clay-mineral particles (E–E: edge–edge clay-mineral contacts; E–F: edge–face clay-mineral contacts). Inter-floc pores may be formed from inter-locking flocs or from the interaction of flocs and silt grains. Much larger ('lacunar') pores are formed by the interaction of either multiple flocs alone, multiple flocs and silt grains, or interactions of silt grains. The components creating the pore are expected to exert a direct control on the response of the pore to mechanical compaction; pores created by flocs alone would be expected to collapse much more readily than those formed wholly by silt and sand grains. Given the way in which muds are deposited, from unsorted flocs or sortable silt, the ideas of Nagaraj *et al.* (1990) provide a potentially direct link between the depositional texture of mud and a description of the pore system.

Fiès (1992) conducted experiments in which silt and fine sand grains of various diameters were mixed with water and different proportions of clay particles to form clay-silt slurries, and then dried under ambient stress conditions. The pore-size distributions of the dried slurries were then determined by MIP. Although these experiments differ from the real depositional systems in that the drying process will lead to shrinkage, they do give us some useful insights into the possible nature of pore systems of muds at deposition.

Based on Fiès' (1992) experiments, the modal diameter of the lacunar pore (LP) size of the dried slurries as a function of (1) their clay content and (2) the size of the silt material added to the clay particles are shown in Figure 2. For the clay-sand mixture, the modal LP size remains virtually constant irrespective of clay content; for the silt-clay mixtures, however, once clay contents exceed 30%, the modal LP size reduces as clay content increases. At clay contents of $<30\%$, the modal LP size is constant, but becomes smaller as the grain size of the silt decreases. Similarly, the modal LP size of materials with clay contents $>30\%$ also reduce as the grain size of the admixed silt decreases.

The apparent change in behavior at clay contents of $\sim 30\%$ suggests a change in the support network of the materials, implying that at smaller clay contents the proportion of silt/sand particles is sufficiently high that the particles interact and provide a framework which allows the formation of a network of larger pores, the size of which depends on the particle size of the (sub-spherical) silt or sand grains. At clay contents $>\sim 30\%$, the clay-particle matrix becomes increasingly influential, silt particles are more dispersed, and the modal size of LP decreases. Fiès (1992) argued that lacunar pores are present

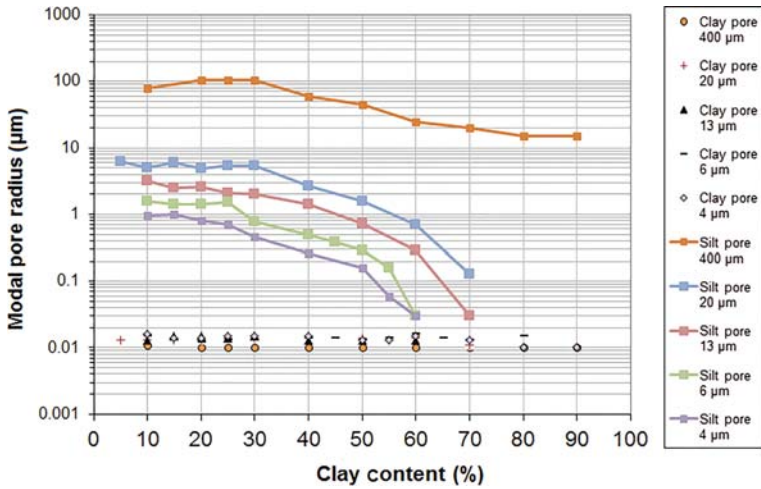


Figure 2. Modal radius of the ‘lacunar’ (LP) and ‘clay’ pore positions in the Fiès (1992) experiments on dried clay-silt slurries, plotted as a function of clay content. Lines represent the modal position of the clay-silt mixtures, plotted according to size of silt particles (400 μm ; 20 μm ; 13 μm ; 6 μm , and 4 μm). Note that at >30% clay content, the position of the modal LP pore size decreases, merging with the clay mode at greater clay fractions. The modal position of the clay pores is constant and independent of clay content.

even at very high clay contents, but are hidden from MIP measurements by the dominance of small pores formed by individual clay particles. Another possibility is that they simply do not exist when the clay contents are large. Note that the modal pore size of the clay pores in these experiments is $\sim 10\text{--}20$ nm.

The pore-size data from Dewhurst *et al.* (1998, 1999a) for natural, Tertiary London Clay mudstones which were compacted experimentally to 33 MPa from their pre-consolidation stress of 1.5–2 MPa, consistent with ~ 200 m burial, are shown in Figure 3. In their initial state, these samples represent shallow-buried mudstones with different clay fractions. Samples with clay fractions >30–40% have unimodal pore-size distributions with the majority of pores below 100 nm. Coarser samples, with clay contents of 27 and 33%, exhibit complex, tri-modal pore-size distributions in their initial, pre-consolidation state. Pores smaller than 50 nm are common and are assumed to relate to the clay fabric, but substantial pore-size modes also exist at ~ 5000 nm and 800 nm, which are the equivalent of the LP suggested by Nagaraj *et al.* (1990) and were also observed in the Fiès (1992) experiments. These larger pores thus relate to the physical framework provided by the larger (> 10 μm), interacting silt grains. The larger pore system is suggested to only occur when the clay fraction is <30–35% of the ‘grain-size distribution.’ At lower clay fractions, the muds can be considered as being framework-supported, and matrix-supported at higher clay fractions. Similar observations have been made by Marion *et al.* (1992), who measured the sonic velocities of clay-sand mixtures, noting a change in behavior at clay fractions above and below $\sim 30\%$, considered to represent the change from matrix to framework support.

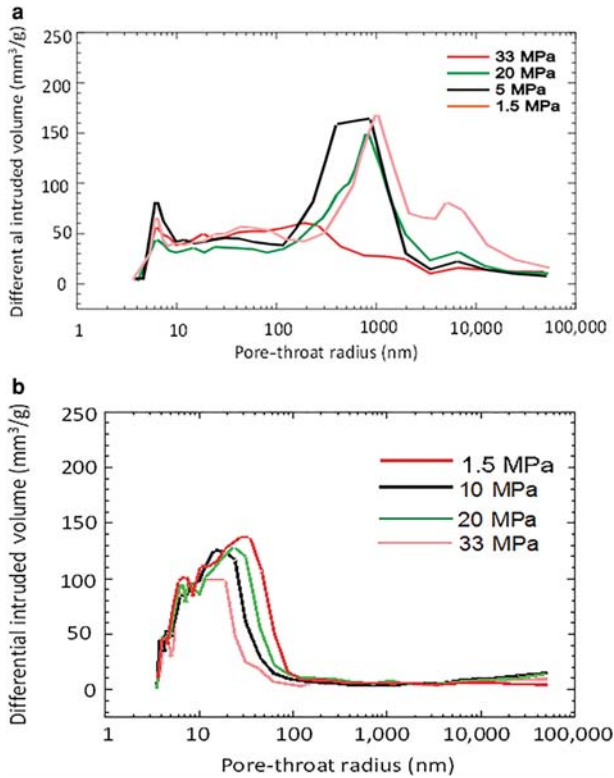


Figure 3. Differential pore-size distribution curves for a silt-rich and a clay-rich sample, both naturally over consolidated to $\sim 1.5\text{--}2$ MPa and then compacted experimentally to 33 MPa: (a) silt-rich sample (27% clay); (b) clay-rich sample (65% clay) (adapted from Dewhurst *et al.*, 1999b).

have been generated in recent years through studies of organic-rich mudstones, *i.e.* shale gas/oil reservoirs. The sum of pore volumes measured by (1) CO_2 sorption at -78°C and (2) MIP, were similar to the total porosity in a set of organic-rich Posidonia shales (Rexer *et al.*, 2014). As mercury occupies pores with constrictions $>\sim 6$ nm, Rexer *et al.* (2014) suggested that porosity measured by CO_2 adsorption at -78°C is largely within pores with effective diameters of <6 nm. CO_2 adsorption experiments at 0°C further suggested that around half of the porosity probed at -78°C was in ultramicropores, *i.e.* pores $<\sim 1$ nm in size, similar to the results of Clarkson *et al.* (2013) from a series of North American gas shales. By experimenting on both shales and isolated kerogens, Rexer *et al.* (2014) were able to show that approximately half of the CO_2 sorption in dry Posidonia shales was in organic matter, with the rest probably associated with clay minerals. As these shales comprise ~ 10 wt.% organic matter and 30 wt.% clay minerals, the proportion of microporosity associated with clay minerals in more

Compaction proceeds primarily by loss of the larger pores, as both silt and clay grains are forced closer together (Figure 3) (Dewhurst *et al.*, 1998, 1999a). At burial depths of 2 km, corresponding to an effective stress of ~ 20 MPa, pore-size distributions of mudstones with clay contents of $<30\%$ are very broad, ranging from sub-20 nm pores associated with the clay-rich parts of the material to micrometer-sized pores related to the silt-rich superstructure of the rock (Figure 1). Pore-size distributions of clay-rich mudstones, as measured by MIP, are not radically different from those from lower effective stresses; small pores have already become even smaller (Figure 1).

Insights into the importance of microporosity and ultramicroporosity in deeply-buried mudstones

common, clay-rich and organic-lean mudstones, will be larger. This is supported by low-pressure CO₂ sorption experiments on pure clay minerals, showing them to be highly microporous (Ross and Bustin, 2009).

While the clay-rich parts of deeply-buried natural mudstones primarily have pore throats smaller than (say) 10 nm, pore ‘bodies,’ as observed by BIB-SEM or FIB-SEM, or probed using low-pressure gas sorption, small-angle and ultra-small-angle neutron scattering (SANS and USANS), can be much larger (*e.g.* Desbois *et al.*, 2009; Heath *et al.*, 2011; Klaver *et al.*, 2012; Clarkson *et al.*, 2012, 2013; Ruppert *et al.*, 2013; Yang *et al.*, 2014), *e.g.* in pressure shadows or at the interfaces of clay aggregates. This illustrates the fundamental difference between observing pore systems using microscopy, which emphasizes pore bodies, and MIP, which emphasizes pore throats. All of these studies also suggest that the distribution of both pore body and pore-throat sizes approximate to power law functions over a range of diameters from nanometer to micrometer. For example, comparison of MIP data with SANS/USANS or BIB-SEM data suggests that in clay-rich, matrix-supported mudstones, any larger (*e.g.* >50 nm) pore bodies are only connected through a network of pore throats with diameters of <~10 nm (Klaver *et al.*, 2012; Clarkson *et al.*, 2013). This accounts readily for the low (nanoDarcy) permeability of clay-rich mudstones compared to silt-rich mudstones (Yang and Aplin, 2010) and illustrates the importance of differentiating between fluid-storage and fluid-flow properties, *e.g.* in the context of hydrocarbon production from shales.

4. Pore size and permeability

Mudstone permeabilities are typically nanoDarcy to microDarcy and are thus difficult and time-consuming to measure (see Neuzil, 1994; Dewhurst *et al.*, 1999b for reviews; also Yang and Aplin, 2007). The MIP data, converted into pore size and shapes using various assumptions, have thus been used widely as a way of estimating permeability rapidly (Leonards, 1962; Scheidegger, 1974; Garcia-Bengochea *et al.*, 1979; Pittman, 1992; Yang and Aplin, 1998). The rationale for the approach is that MIP is a measure of the size and connectivity of pore throats. One approach, commonly used for sandstones, uses the Kozeny-Carman equation, which assumes that pores are bundles of capillary tubes. The equation requires poorly-defined “shape” and “tortuosity” factors which are poorly constrained in mudstones. Based on MIP data on 30 mudstone samples which were also measured for permeability, Yang and Aplin (2007) calculated values of 200 and 1000 as the products of the shape and the tortuosity factors for horizontal and vertical permeabilities, respectively. These values are much greater than those typically used for sandstones and reflect the complexity and relatively poor connectivity of mudstone pore systems, compared to sand.

The measured permeability data to calibrate an earlier pore-based permeability model, in which pores were assumed to have the shape of two frustra of cones, connected at their base were also used by Yang and Aplin (2007). Pores were assumed to be flatter in mudstones with greater clay contents, and also to flatten with increasing

stress. The model was able to predict the measured permeabilities to within \pm a factor of 3 of the true value. The idea that pores in clay-rich mudstones are relatively flat, thus reflecting the shape of clay grains, is intuitively reasonable and has, to some extent, been validated by recent 3D images from the FIB-SEM (e.g. Desbois *et al.*, 2009; Heath *et al.*, 2011).

While permeability estimates based on MIP data may be reasonable for homogeneous mudstones, they are inappropriate for heterogeneous mudstones, e.g. laminated mudstones comprising clay-silt couplets. This reflects the fact that MIP is an omnidirectional technique, whereas permeability measurements are unidirectional, generally vertical or horizontal. As silt-rich mudstones can be three orders of magnitude more permeable than clay-rich mudstones (Dewhurst *et al.*, 1998; Yang and Aplin, 2010), laminated, heterogeneous mudstones are expected to be highly anisotropic, and have been shown to have k_h/k_v ratios in excess of 10^3 (Armitage *et al.*, 2011). Estimates of directional permeability would need to be based on directional MIP data. These points emphasize the need to combine and integrate MIP analyses with microscopy or SANS techniques, if appropriate interpretations are to be made regarding pore bodies and pore connectivity.

As an example, the bimodal nature of a pore-size distribution which is interpreted to reflect the fine-scale, sedimentological structure of the sample rather than an intrinsic property of an homogenous mudstone lithology is shown in Figure 4. The more clay-rich

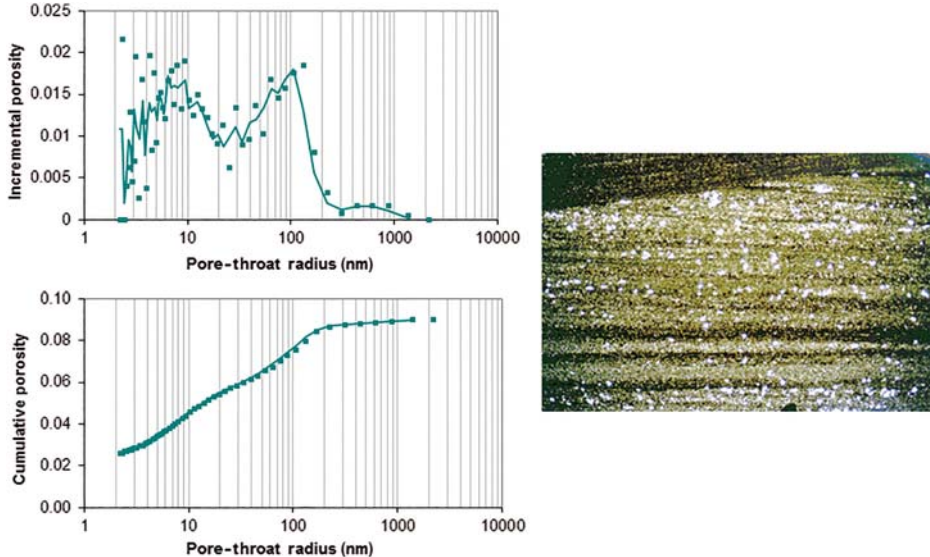


Figure 4. Combined Mercury Injection Capillary Pressure (MICP) and microscopy analysis: (upper and middle) differential and cumulative pore-size distribution curves for a silt-rich natural mudstone; (lower) transmitted-light photomicrograph (plane-polarized light) of the same sample exhibiting low-angle lamination; the laminae have sharp upper and lower contacts indicating the actions of bottom currents. The field of view is 2.7 mm across.

parts of the sample (darker brown in Figure 4) will be dominated by pores with throats of $< \sim 10$ nm, whereas the more silt-rich parts of the sample comprise mainly pores with throats of $> \sim 50$ – 100 nm. A heterogeneity, therefore, exists which would result in a highly anisotropic permeability on the observed sample scale; this may or may not be reflected at larger scales, depending on the larger-scale connectivity of the two distinct parts of the sample. Such connectivity, for example, could be studied using micro-CT methodologies and is critical for understanding the permeability structure of shale reservoirs and cap rocks.

More work is clearly needed to develop a detailed understanding of the way in which the pore systems of fine-grained sediments evolve as functions of lithology, compaction, and diagenesis. The inevitable complexity of pore systems means that considering some relatively simple rules which allow predictive fluid-storage and fluid-flow models to be developed on scales larger than those that can be measured under the microscope or in the laboratory would, however, be useful. For mudstones, as shown here, a division between matrix-supported (clay-rich) and framework-supported (silt-rich) materials is a useful simplification. Silt-clay couplets are common depositional features of mudstones, so that this simple approach not only ties back pore systems to the depositional environment of the host materials but can also be used to produce building blocks for further upscaling of fluid-storage and fluid-flow properties.

5. Conclusions

Grains within siliciclastic muds are deposited either as flocs, in which grains are generally $< \sim 10$ μm , and single grains: “sortable silt”, generally > 10 μm . Mineralogically, the majority of sub- 10 μm grains are phyllosilicates, while the majority of > 10 μm grains are quartz, feldspars, and micas.

Based primarily on MIP data, pore-throat sizes within clay-rich mudstones are commonly < 20 nm, even at burial depths of 100 m. Analysis of the grain-size and pore-size distributions of muds and mudstones suggests that when clay-size (< 2 μm diameter) particles form $> 30\%$ of the mudstone, pore-size distributions are controlled by the interaction of clay minerals; these materials are ‘matrix-supported.’ Continued compaction simply reduces the modal pore size of the porosity to smaller values, such that a large fraction of the clay-related porosity is within pores of < 10 nm in samples buried to > 2 km. When clay-size particles comprise $< \sim 30\%$ of the ‘grain-size distribution,’ a second, much larger pore system is observed, controlled by the amount and size of sortable silt; these mudstones are ‘framework-supported.’ Compaction of these silt-rich materials occurs mainly by the loss of the largest pores, but large pores still exist up to high effective stresses in the absence of chemical compaction.

Mercury injection porosimetry provides information about pore-throat size and pore connectivity and thus provides useful data with which to estimate permeability. Models based on generally flat pore shapes can estimate the permeability of homogenous

mudstones to \pm a factor of 3 of the true value, but cannot be used for heterogeneous, laminated mudstones, which have permeability anisotropies of up to and beyond 10^3 .

Because MIP gives information about pore throats whereas microscopy gives information about pore bodies and about the sedimentological fabric of the sample, it is inevitable but enriching that the two techniques generate different results. Both are required, along with other techniques such as SANS and low-pressure gas sorption, in order to fully appreciate the complexity of mudstone pore systems.

Because silt-clay couplets are common depositional features of mudstones, and silt-rich and clay-rich units have very different pore systems, a simple division between silt-rich and clay-rich can be used to produce building blocks for further upscaling.

Acknowledgments

The present work was funded largely by the Caprocks JIP, comprising Anadarko, BG Group, BHPBilliton, BP, Chevron, ConocoPhillips, ENI, ExxonMobil, Petrobras, Shell, Statoil, and Total; thanks to all.

Guest editor: H.C. Greenwell

The authors and editors are grateful to anonymous reviewers who offered very helpful input and suggestions. A list of all reviewers is given at the end of the Preface for this volume.

References

- Allredge, A.L. and Silver, M.W. (1988) Characteristics, dynamics and significance of marine snow. *Progress in Oceanography*, **20**, 41–82.
- Armitage, P.J., Faulkner, D.R., Worden, R.H., Aplin, A.C., Butcher, A.R., and Illiffe, J. (2011) Experimental measurement of, and controls on, permeability and permeability anisotropy of caprocks from the CO₂ storage project at the Krechba Field, Algeria. *Journal of Geophysical Research*, **116**, B12208, doi: 10.1029/2011JB008385.
- Borst, R.L. (1982) Some effects of compaction and geological time on the pore parameters of argillaceous rocks. *Sedimentology*, **29**, 291–298.
- Clarkson, C.R., Freeman, M., He, L., Agamalian, M., Melnichenko, Y.B., Mastalerz, M., Bustin, R.M., Radliński, A.P., and Blach, T.P. (2012) Characterization of tight gas reservoir pore structure using USANS/SANS and gas adsorption analysis. *Fuel*, **95**, 371–385, doi: 10.1016/j.fuel.2011.12.010.
- Clarkson, C.R., Solano, N., Bustin, R.M., Bustin, A.M.M., Chalmers, G.R.L., He, L., Melnichenko, Y.B., Radliński, A.P., and Blach, T.P. (2013) Pore structure characterization of North American shale gas reservoirs using USANS/SANS, gas adsorption, and mercury intrusion. *Fuel*, **103**, 606–616, doi: 10.1016/j.fuel.2012.06.119
- Curran, K.J., Hill, P.S., and Milligan, T.G. (2002) Fine-grained suspended sediment dynamics in the Eel River flood plume. *Continental Shelf Research*, **22**, 2537–2550.
- Curran, K.J., Hill, P.S., Schell, T.M., Milligan, T.G., and Piper, D.J.W. (2004) Inferring the mass fraction of flocc-deposited mud: application to fine-grained turbidites. *Sedimentology*, **51**, 927–944.
- Desbois, G., Urai, J.L., and Kukla, P.A. (2009) Morphology of the pore space in claystones – evidence from BIB/FIB ion beam sectioning and cryo-SEM observations. *Earth*, **4**, 15–22.

- Dewhurst, D.N., Aplin, A.C., Sarda, J.P., and Yang, Y.L. (1998) Compaction-driven evolution of porosity and permeability in natural mudstones: An experimental study. *Journal of Geophysical Research – Solid Earth*, **103**, 651–661.
- Dewhurst, D.N., Aplin, A.C., and Sarda, J.P. (1999a) Influence of clay fraction on pore-scale properties and hydraulic conductivity of experimentally compacted mudstones. *Journal of Geophysical Research – Solid Earth*, **104**, 29261–29274.
- Dewhurst, D.N., Yang, Y.L., and Aplin, A.C. (1999b) Permeability and fluid flow in natural mudstones. Pp. 23–43 in: *Muds and Mudstones: Physical and Fluid Flow Properties* (A.C. Aplin, A.J. Fleet, and J.H.S. Macquaker, editors). Geological Society Special Publication, **158**, The Geological Society, London.
- Eisma, D. and Li, A. (1993) Changes in suspended-matter floc size during the tidal cycle in the Dollard estuary. *Netherlands Journal of Sea Research*, **31**, 107–117.
- Fiès, J.C. (1992) Analysis of soil textural porosity relative to skeleton particle size, using mercury porosimetry. *Soil Science Society of America Journal*, **56**, 1062–1067.
- García-Bengochea, I., Lovell, C.W., and Althaeffl, A.G. (1979) Pore distribution and permeability of silty clays. *Journal of Geotechnical Engineers Division, Proceedings ASCE*, **105**, 839–856.
- Heath, J.E., Dewers, T.A., McPherson, B.J.O.L., Petrusak, R., Chidsey, T.C., Rinehart, A.J., and Mozley, P.S. (2011) Pore networks in continental and marine mudstones: characteristics and controls on sealing behaviour. *Geosphere*, **7**, 429–454.
- Klaver, J., Desbois, G., Urai, J.L., and Littke, R. (2012) BIB-SEM study of the pore space morphology in early mature Posidonia Shale from the Hils area, Germany. *International Journal of Coal Geology*, **103**, 12–25.
- Kranck, K. (1973) Flocculation of suspended sediment in sea. *Nature*, **246**, 348–350.
- Kranck, K. (1975) Sediment deposition from flocculated suspensions. *Sedimentology*, **22**, 111–123.
- Kranck, K. and Milligan, T.G. (1985) Origin of grain-size spectra of suspension deposited sediment. *Geo-Marine Letters*, **5**, 61–66.
- Kranck, K., Smith, P.C., and Milligan, T.G. (1996a) Grain-size characteristics of fine-grained unflocculated sediments. 1. ‘One-round’ distributions. *Sedimentology*, **43**, 589–596.
- Kranck, K., Smith, P.C., and Milligan, T.G. (1996b) Grain-size characteristics of fine-grained unflocculated sediments. 2. ‘Multi-round’ distributions. *Sedimentology*, **43**, 597–606.
- Leonards, G.H. (1962) *Engineering Properties of Soils*. McGraw-Hill, New York.
- Marion, D., Nur, A., Yin, H., and Han, D. (1992) Compressional velocity and porosity in sand-clay mixtures. *Geophysics*, **57**, 554–563.
- McCave, I.N., Manighetti, B., and Robinson, S.G. (1995) Sortable silt and fine sediment size composition slicing – parameters for paleocurrent speed and paleoceanography. *Paleoceanography*, **10**, 593–610.
- Nagaraj, T.S., Griffiths, F.J., Joshi, R.C., Vatsala, A., and Murthy, B.R.S. (1990) Change in pore-size distribution due to consolidation of clays – discussion. *Geotechnique*, **40**, 303–309.
- Neuzil, C.E. (1994) How permeable are clays and shales. *Water Resources Research*, **30**, 145–150.
- Pittman, E.D. (1992) Relationship of porosity and permeability to various parameters derived from mercury injection-capillary pressure curves for sandstone. *American Association of Petroleum Geologists Bulletin*, **76**, 191–198.
- Rexer, T.F.T., Mathia, E.J., Aplin, A.C., and Thomas, K.M. (2014) High-pressure methane adsorption and characterization of pores in Posidonia shales and isolated kerogens. *Energy Fuels*, **28**, 2886–2901. DOI: 10.1021/ef402466m.
- Ross, D.J.K. and Bustin, R.M. (2009) The importance of shale composition and pore structure upon gas storage potential of shale gas reservoirs. *Marine and Petroleum Geology*, **26**, 916–927.
- Ruppert, L.F., Sakurovs, R., Blach, T.P., He, L., Melnichenko, Y.B., Mildner, D.F.R., and Alcantar-Lopez, L. (2013) A USANS/SANS study of the accessibility of pores in the Barnett Shale to methane and water. *Energy Fuel*, **27**, 772–779, doi: 10.1021/ef301859s
- Scheidegger, A.E. (1974) *The Physics of Flow through Porous Media*, 3rd edition. University of Toronto Press, Toronto.

- Schlömer, S. and Krooss, B.M. (1997) Experimental characterisation of the hydrocarbon sealing efficiency of cap rocks. *Marine and Petroleum Geology*, **14**, 563–578.
- Stumm, W. and Morgan, J.J. (1995) *Aquatic Chemistry: Chemical Equilibria and Rates in Natural Waters*. Environmental Science and Technology, Wiley, New York.
- Yang, F., Ning, Z., and Liu, H. (2014) Fractal characteristics of shales from a shale gas reservoir in the Sichuan Basin, China. *Fuel*, **115**, 378–384, doi: 10.1016/j.fuel.2013.07.040
- Yang, Y.L. and Aplin, A.C. (1998) Influence of lithology and compaction on the pore size distribution and modelled permeability of some mudstones from the Norwegian margin. *Marine and Petroleum Geology*, **15**, 163–175.
- Yang, Y.L. and Aplin, A.C. (2007) Permeability and petrophysical properties of 30 natural mudstones. *Journal of Geophysical Research – Solid Earth*, **112**, B03206, doi: 10.1029/2005JB004243.
- Yang, Y.L. and Aplin, A.C. (2010) A permeability-porosity relationship for mudstones. *Marine and Petroleum Geology*, **27**, 1692–1697, doi: 10.1016/j.marpetgeo.2009.07.001